

PCCP

Accepted Manuscript



This is an *Accepted Manuscript*, which has been through the Royal Society of Chemistry peer review process and has been accepted for publication.

Accepted Manuscripts are published online shortly after acceptance, before technical editing, formatting and proof reading. Using this free service, authors can make their results available to the community, in citable form, before we publish the edited article. We will replace this *Accepted Manuscript* with the edited and formatted *Advance Article* as soon as it is available.

You can find more information about *Accepted Manuscripts* in the [Information for Authors](#).

Please note that technical editing may introduce minor changes to the text and/or graphics, which may alter content. The journal's standard [Terms & Conditions](#) and the [Ethical guidelines](#) still apply. In no event shall the Royal Society of Chemistry be held responsible for any errors or omissions in this *Accepted Manuscript* or any consequences arising from the use of any information it contains.



Physical Chemistry Chemical Physics

COMMUNICATION

Pressure-induced Mesoscopic Disorder in Protic Ionic Liquids: First Computational Study.

Received 00th January 20xx,
Accepted 00th January 20xx

A. Mariani,^{*a} R. Caminiti,^a M. Campetella^a and L. Gontrani^a

DOI: 10.1039/x0xx00000x

www.rsc.org/

It has been recently shown that pressure may affect the mesoscopic heterogeneity in Aprotic Ionic Liquids, owing to the long alkyl chain folding on itself. Here we explore Protic Ionic Liquids, using Classical Molecular Dynamics. These compounds have shorter and stiffer alkyl chains, harder to fold. We observed that high pressures affects the mesoscopic structure of the studied chemicals and, indeed, the effect may be ascribed to chain folding.

Ionic Liquids (ILs) are among the most studied compounds nowadays¹, due to their chemical and physical properties^{2–5} that can be tuned via chemical substitutions on the anion and/or the cation. A remarkable feature of ILs is their micro-heterogeneity^{6–11} arising from the segregation of two domains: one polar domain made up of anions and charged heads of cations and another apolar domain composed of cationic alkyl tails. This organization leads to the characteristic “low q peak” (LqP) in the Small Angle X-Ray Scattering (SAXS) patterns of ILs. The LqP is generally attributed to the separation of two anions¹² and, therefore, to the apolar domain size in between them. Mixing of a co-solvent could change the relative dimensions of the two domains and may sometimes lead to some interesting observations like clustering¹³ and formation of stoichiometric complexes¹⁴, while other mixtures results in a homogenous state¹⁵. ILs can be divided into Protic (PILs) and Aprotic (APILs) liquids. Two of the most important differences between them are that PILs can build up an extended 3D network of hydrogen bonds similar to water¹⁶, and that the LqP in the SAXS pattern for PILs is visible even when the alkyl chain is just two carbon atoms long¹⁷, on the other hand in APILs a length of at least four carbons seems to be required⁶, or at least no LqP has been yet reported for APILs with shorter chains. Recently, Yoshimura *et al.*¹⁸ have observed that the application of high pressures to the APIL 1-octyl-3-methyl-

imidazolium tetrafluoroborate leads to progressive vanishing of the LqP, suggesting that the anion separation decreases (i.e. the apolar domain is contracted). Soon after, Russina *et al.*¹⁹ carried out some Molecular Dynamics Simulations on the same system as a function of pressure and explained this behaviour in terms of the long alkyl chains folding²⁰, inducing homogenization of the system and reducing the dispersive forces. If this is a general behaviour, ILs with smaller alkyl chains should exhibit less response to enhanced pressure. In this work we have chosen three PILs, viz. Ethylammonium Nitrate (EAN), Propylammonium Nitrate (PAN) and Butylammonium Nitrate (BAN), because all of them show the LqP and have short chains^{21–23}. A schematic representation of these PILs is provided in Figure 1. The effect of the pressure on the structure was explored by means of Classical Molecular Dynamics Simulations, as described in the Computational Methods section. Each system was simulated at four different pressure values: 100 kPa, 100 MPa, 500 MPa and 1 GPa. At these pressures, all the samples are liquid at room temperature, as reported by Capitani *et al.*²⁴. The reliability of the models was checked by comparison of the computed densities with the respective experimental ones at room pressure and the agreement was found to be good for all the three PILs (see Table 1); moreover, a comparison between the experimental and computed Wide Angle X-ray Scattering (WAXS) patterns of the PILs at room pressure confirmed the goodness of the models (see Figure 2). For higher pressure values no data for densities or WAXS are yet available, notwithstanding that, we computed the theoretical densities of the systems as a function of pressure, and the results are shown in Figure 3. The structure function $I(q)$ was computed for all the models and valuable differences in the LqP were consequently observed (see Figure 4). It appears clear that LqP is gradually shifted to higher q values and its intensity is decreased. The shift may be ascribed to the compression of the apolar domain in response to the pressure. The intensity loss may be explained by progressive disordering of the molecules within the box, i.e. the PILs have no more their native “sponge like” structure. The same effect is observed in

^a Department of Chemistry, “La Sapienza” University of Rome, P.le Aldo Moro 5, 00185 Rome, Italy.

E-mail: alessandro.mariani@uniroma1.it

E-mail: ruggero.caminiti@uniroma1.it

E-mail: marco.campetella@uniroma1.it

E-mail: lorenzo.gontrani@uniroma1.it

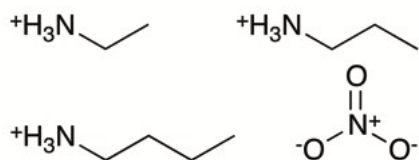


Figure 1. Schematic representation of the Protic Ionic Liquids dealt with in this work. From left top to right bottom: Ethylammonium, Propylammonium and Butylammonium cations, Nitrate anion.

Table 1. Comparison between experimental and computed densities.

| Ionic Liquid | Experimental [g/cc] | Computed [g/cc] |
|--------------|---------------------|-----------------|
| EAN | 1.21 | 1.2143 |
| PAN | 1.16 | 1.1596 |
| BAN | 1.10 | 1.0938 |

Experimental values was provided in literature by Atkin *et al.*⁷ for EAN and PAN, and by Xu *et al.*²⁵ for BAN.

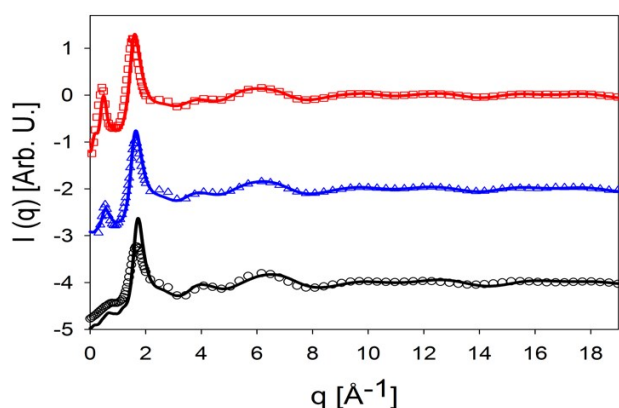


Figure 2. Wide Angle X-ray Scattering patterns for EAN (black), PAN (blue) and BAN (red). The symbols are for experimental data. The EAN and BAN experimental patterns was provided in literature by Caminiti *et al.*^{23,26}. For PAN we have collected the WAXS pattern as described in the Experimental Methods section.

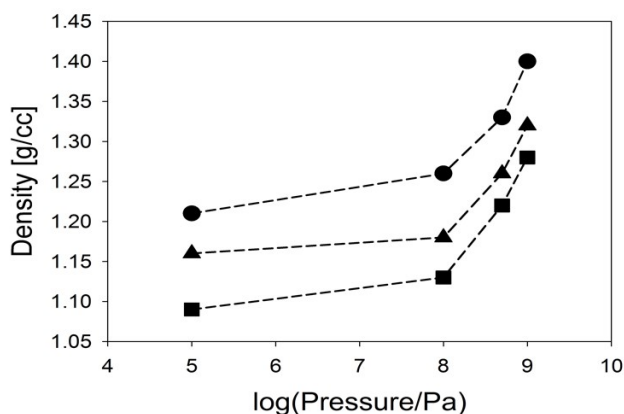


Figure 3. Computed densities as a function of pressure. EAN (circles); PAN (triangles); BAN (squares).

binary mixtures of such compounds with some molecular solvents like water¹⁵, so the pressure rising is an event that induces disorder in ILs as mixing does. The magnitude of the effect on the LqP follows the order BAN>PAN>>EAN, in agreement with the interpretation of alkyl chain folding.

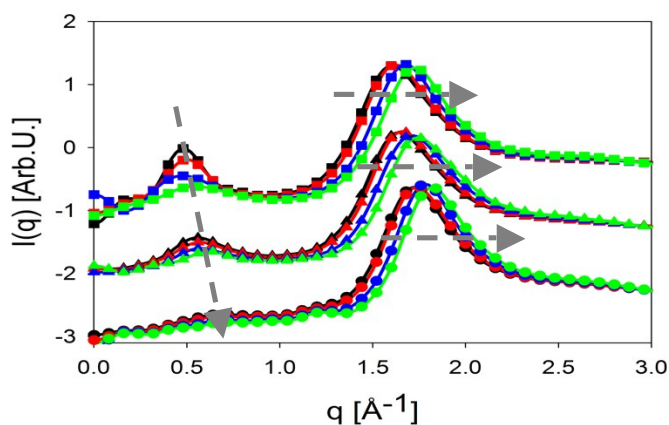


Figure 4. Computed SAXS patterns for analysed systems. EAN (circles); PAN (triangles); BAN (squares). 100kPa (black); 100 MPa (red); 500 MPa (blue); 1GPa (green).

On the other hand, the main peak between 1.5 \AA^{-1} and 2 \AA^{-1} is just shifted to higher q values while maintaining its intensity. Therefore, shorter correlations responsible for this peak, are not dramatically affected by the increased pressure and they appear to be just shrunk. EAN has a barely visible LqP in SAXS, but it has been reported¹⁰ that this feature is quite stronger in Neutron Diffraction, so we have computed the Small Angle Neutron Scattering (SANS) pattern for ammonium deuterated EAN (d3-EAN) as a function of pressure and the results are reported in Figure 5. The room pressure pattern qualitatively reproduces the experimental pattern reported by some of us²⁶. As can be seen the effect of the pressure on the LqP is quite weak, as can be expected considering that a two-carbon chain cannot fold. The separation of the structure functions into anion-anion and cation-cation components (see Figure 6), allows to unambiguously confirm that the LqP is almost completely due to anion-anion long range correlations; this may suggest once more that the alkyl chain folding theory can be applied. In Figure 6 EAN is not presented because the effect of pressure is negligible. Of course, a two-carbon chain cannot be folded and, therefore, only slight effects at very high pressures can be observed in EAN. This fact is a quite strong confirmation that the "scorpion" model by Shimizu *et al.*²⁰, is a good interpretation. To check the molecular organization within the boxes, Classical Molecular Dynamics Simulations analysis was carried out using the TRAVIS software²⁷. A direct measure of the chain folding may be achieved following several structural changes. We have selected the most appropriate one for each different PIL in this work upon their structural characteristics: for EAN we used the $C_{\text{terminal}} - N_{\text{cation}}$ Pair Distribution Function (PDF), the $C_{\text{terminal}} - C_2 - C_1 - N_{\text{cation}}$ dihedral angle distribution for PAN and $C_{\text{terminal}} - C_2 - N_{\text{cation}}$ angular distribution for BAN, Figure 7. As it can be expected, the PDF in Figure 7 show a single sharp peak for EAN which is unaffected by the pressure change because a two-atom chain cannot fold. For PAN three peaks appear in the dihedral distribution: the highest one at 180° is due to the completely elongated chain, the two other peaks (50° and 290°) are due to folded chain. At 1 GPa it is evident how the peak of the elongated form has a decreased intensity while the other two are enhanced. For BAN angular distribution, a similar, yet more

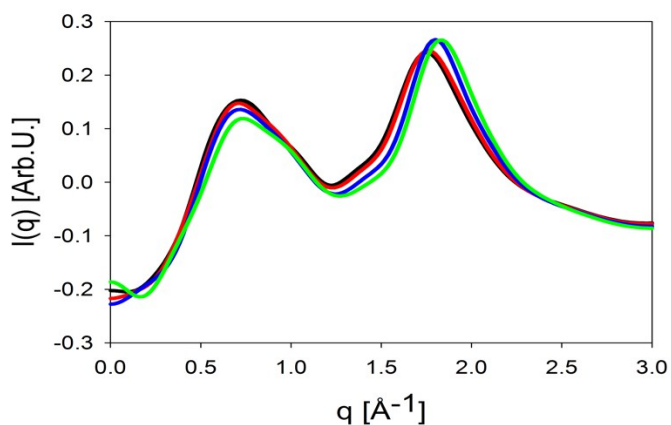


Figure 5. Computed SANS pattern for ammonium deuterated EAN. 100 kPa (black); 100 MPa (red); 500 MPa (blue); 1 GPa (green).

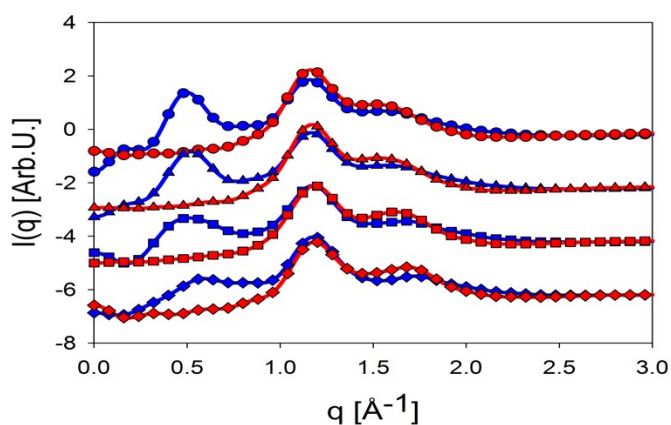
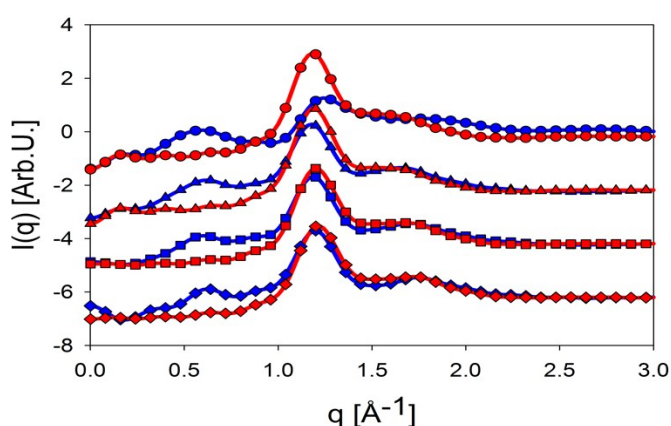


Figure 6. Computed partial structure functions. Anion-anion (blue); cation-cation (red). 100 kPa (circles); 100 MPa (triangles); 500 MPa (squares); 1 GPa (diamonds). PAN (top); BAN (bottom)

extreme scenario can be observed. There are three peaks, each of them can be linked to a different conformer of the chain: a fully elongated form at $\sim 180^\circ$, a partially folded one at $\sim 120^\circ$, and fully folded at $\sim 95^\circ$. The pressure effect leads to a decrease of the intensity of the peak associated with the elongated form, while enhancing the other two, as it is expected. In Figure 8 the three forms associated with the peaks in BAN $C_{\text{terminal}}-C_2-N_{\text{cation}}$ angular distribution function are reported. Some Spatial Distribution Functions were

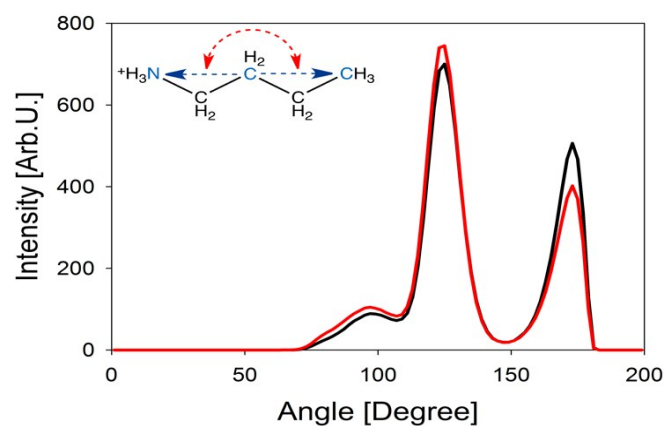
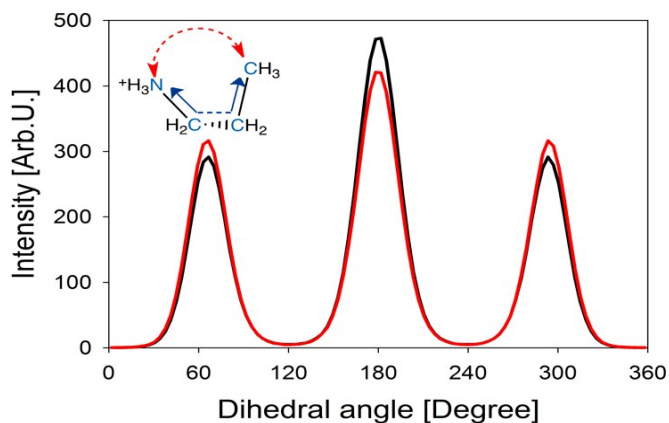
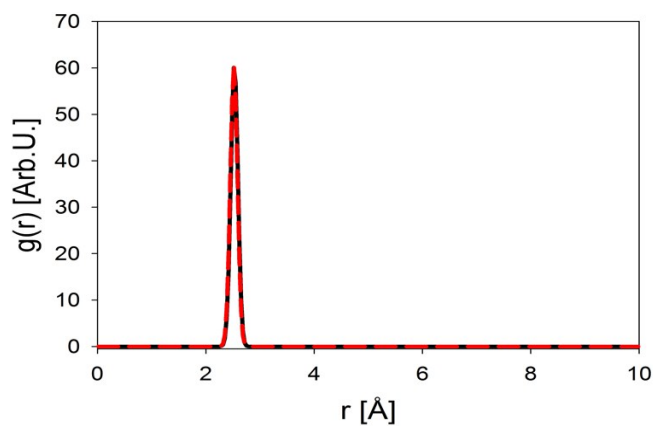


Figure 7. Structural changes in the analysed compounds. $C_{\text{terminal}}-N_{\text{cation}}$ pair distribution function for EAN (top); the $C_{\text{terminal}}-C-C_1-N_{\text{cation}}$ dihedral angle distribution for PAN, schematic representation of the angle in the insert (middle); $C_{\text{terminal}}-C_2-N_{\text{cation}}$ angular distribution for BAN, schematic representation of the angle in the insert (bottom).

computed and the results achieved for BAN and visualized using the VMD²⁸ 1.9.2 software are shown in Figure 9. The cation aliphatic chain appears to be much less coordinated to other chains at 1 GPa, implying that the apolar domain is no more well defined as at atmospheric pressure. Furthermore, the polar head is more occupied by anions while other polar heads are removed. This suggests that while the ion pair is persistent in all the pressure range, the mesoscopic structure is lost and a near-homogenous, disordered state is reached at

COMMUNICATION

Journal Name

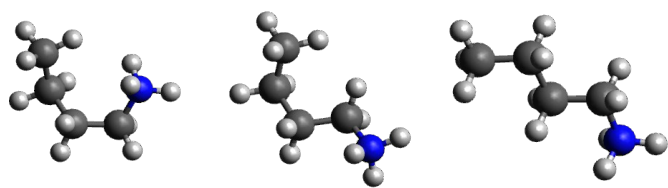


Figure 8. Butylammonium cation conformers associated with the peaks in Figure 7 (bottom). Completely folded form (left) responsible of the broad peak at $\sim 95^\circ$; partially folded form (center) responsible of the central peak at $\sim 120^\circ$; elongated form (right) responsible of the peak at $\sim 180^\circ$.

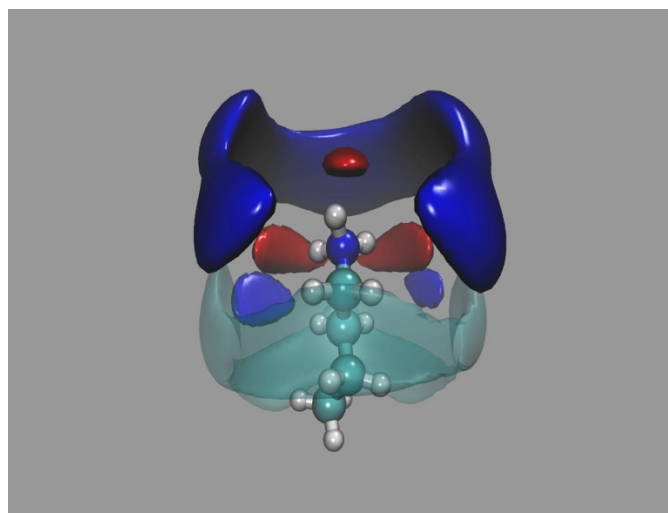
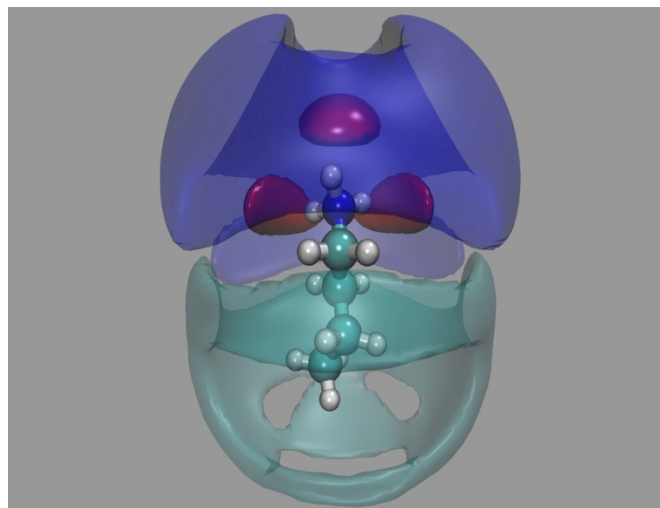


Figure 9. Spatial distribution functions of various atoms around a central butylammonium cation. All the clouds are plotted for an isodensity of 1.7 times the bulk one. Terminal carbon of the cation (cyan); nitrogen of the cation (blue); oxygens of the anion (red). 100 kPa (top); 1 GPa (bottom).

1 GPa. A direct measure of the apolar domains in the studied systems was carried out using the new Voronoi analysis tool developed in TRAVIS software²⁹. We chose all the cation atoms as the base population, while the domain of interest included the terminal ethyl group. The measured average volume of the apolar domain(s) as a function of pressure was then computed and is reported in Figure 10. It appears evident that the effect

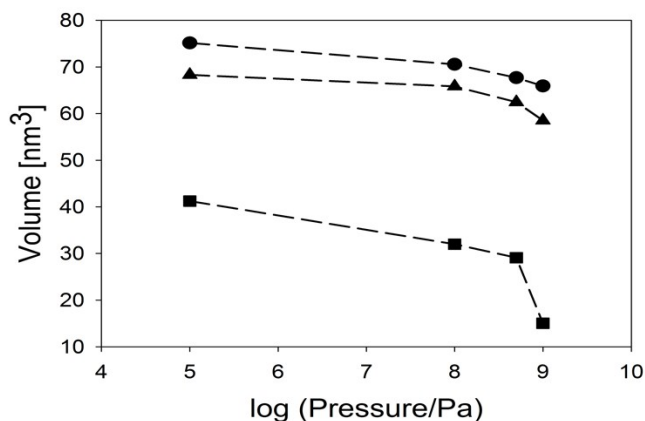


Figure 10. Computed average volume of the apolar domain(s) of BAN (squares), PAN (triangles) and EAN (circles) as a function of pressure.

of pressure on the apolar domain size is much more chain is flexible, the strongest the effect of the pressure on the structure is. Details on this kind of analysis can be found in Ref. 29.

Conclusions

Summarizing, in this work we have explored the effect of pressure on EAN, PAN and BAN, observing a progressive build-up of disorder of the liquid with increasing pressure and a consequent loss of the characteristic mesoscopic ILs domain segregation. Classical Molecular Dynamics Simulations analysis showed that the alkyl chain folding theory can be applied to this kind of systems and it may explain all the observed features. More precisely, a shrunk alkyl chain is not as hydrophobic as a full-elongated one because a ring-like conformation exposes less surface to the environment than a linear structure. Therefore, the compressed cations are no longer able to generate a defined apolar domain. Since this is the very first report on PILs involving high pressures, further inspections are mandatory. We are currently performing simulations on other similar systems to achieve a complete scenario and we are arranging for some diffraction experiments at Large Scale Facilities to get experimental confirmation.

Computational Methods

All the simulations were carried out using AMBER 12³⁰ with GAFF Force Field³¹. Missing parameters, such atom charges for anions and cations, were computed through RESP fitting of the electrostatic potential calculated at the B3LYP/6-311++G** level of theory. A dielectric constant of 1.8 was set because we observed that such a value leads to very good values of the densities for all the systems in this work at room pressure. This is equivalent to scale atom point charges of a factor of ~ 0.75 . For all the simulations a box of 1000 ionic pairs was used with the following procedure: 10^7 minimization cycles; 0.5 ns of NVT at 50 K; 5 ns of equilibration NPT at final pressure; 1 ns productive NPT. For all those phases a timestep of 2 fs was used accordingly with the suggestion of the SHAKE algorithm³².

The DFT calculations were performed using the Gaussian-09 (D1 Version)³³. The calculation of the structure factors and of their Fourier transform was accomplished using g_rdf (GROMACS³⁴ suite) and the in-house software, written by L. Gontrani and R. Caminiti, that implement the formulae reported elsewhere³⁵.

Experimental Methods

The Propylammonium Nitrate was purchased at IoLiTec at the highest available purity ($\geq 97\%$). The sample was dehydrated by pumping it in high vacuum under slight warming (50°C) overnight. The final water concentration was checked by $^1\text{H-NMR}$ and it was undetectable ($\leq 0.5\%$). Then the sample was injected in a 2mm o.d. quartz capillary and the WAXS pattern was collected at room temperature and pressure using the diffractometer projected by Prof. Ruggero Caminiti, located in the Department of Chemistry of "La Sapienza" University of Rome (Italian Patent No. 01126484-23 June, 1993)³⁶. Details on how the data were treated can be found in Ref. 36.

Acknowledgments

The authors thank Prof. Ruggero Caminiti (Sapienza University of Rome Chemistry Department) for providing free usage of Narten computing cluster facility.

References

- 1 T. L. Greaves and C. J. Drummond, *Chem. Rev.*, 2015.
- 2 C. Chiappe and D. Pieraccini, *J. Phys. Org. Chem.*, 2005, **18**, 275–297.
- 3 U. Domańska, *Thermochim. Acta*, 2006, **448**, 19–30.
- 4 E. W. Castner and J. F. Wishart, *J. Chem. Phys.*, 2010, **132**, 120901.
- 5 S. B. Capelo, T. Méndez-Morales, J. Carrete, E. López Lago, J. Vila, O. Cabeza, J. R. Rodríguez, M. Turmine and L. M. Varela, *J. Phys. Chem. B*, 2012, **116**, 11302–12.
- 6 A. Triolo, O. Russina, H.-J. Bleif and E. Di Cola, *J. Phys. Chem. B*, 2007, **111**, 4641–4.
- 7 R. Atkin and G. G. Warr, *J. Phys. Chem. B*, 2008, **112**, 4164–6.
- 8 A. Triolo, O. Russina, B. Fazio, G. B. Appetecchi, M. Carewska and S. Passerini, *J. Chem. Phys.*, 2009, **130**, 164521.
- 9 T. L. Greaves, D. F. Kennedy, S. T. Mudie and C. J. Drummond, *J. Phys. Chem. B*, 2010, **114**, 10022–31.
- 10 R. Hayes, S. Imberti, G. G. Warr and R. Atkin, *Phys. Chem. Chem. Phys.*, 2011, **13**, 3237–47.
- 11 T. L. Greaves and C. J. Drummond, *Chem. Soc. Rev.*, 2013, **42**, 1096–120.
- 12 M. Campetella, L. Gontrani, F. Leonelli, L. Bencivenni and R. Caminiti, *Chemphyschem*, 2015, **16**, 197–203.
- 13 O. Russina, A. Mariani, R. Caminiti and A. Triolo, *J. Solution Chem.*, 2015, **44**, 699–685.
- 14 O. Russina, M. Macchiagodena, B. Kirchner, A. Mariani, B. Aoun, M. Russina, R. Caminiti and A. Triolo, *J. Non. Cryst. Solids*, 2015, **407**, 333–338.
- 15 R. Hayes, S. Imberti, G. G. Warr and R. Atkin, *Angew. Chem. Int. Ed. Engl.*, 2012, **51**, 7468–71.
- 16 K. Fumino, A. Wulf and R. Ludwig, *Angew. Chem. Int. Ed. Engl.*, 2009, **48**, 3184–6.
- 17 Y. Umebayashi, W.-L. Chung, T. Mitsugi, S. Fukuda, M. Takeuchi, K. Fujii, T. Takamuku, R. Kanzaki and S. Ishiguro, *J. Comput. Chem. Japan*, 2008, **7**, 125–134.
- 18 Y. Yoshimura, M. Shigemi, M. Takaku, M. Yamamura, T. Takekiyo, H. Abe, N. Hamaya, D. Wakabayashi, K. Nishida, N. Funamori, T. Sato and T. Kikegawa, *J. Phys. Chem. B*, 2015, **119**, 8146–8153.

COMMUNICATION

Journal Name

- 19 O. Russina, F. Lo Celso and A. Triolo, *Phys. Chem. Chem. Phys.*, 2015, **17**, 12552–12561.
- 20 K. Shimizu, C. E. S. Bernardes, A. Triolo and J. N. Canongia Lopes, *Phys. Chem. Chem. Phys.*, 2013, **15**, 16256–62.
- 21 R. Hayes, S. Imberti, G. G. Warr and R. Atkin, *Phys. Chem. Chem. Phys.*, 2011, **13**, 13544–51.
- 22 L. Gontrani, E. Bodo, A. Triolo, F. Leonelli, P. D. Angelo, V. Migliorati and R. Caminiti, *J. Phys. Chem. B*, 2012, **116**, 13024–13032.
- 23 L. Gontrani, P. Ballirano, F. Leonelli and R. Caminiti in *The Structure of Ionic Liquids, Soft and Biological Matter*; R. Caminiti, L. Gontrani, Eds. Springer International Publishing: Cham, Switzerland, 2014, 20–26.
- 24 F. Capitani, C. Fasolato, S. Mangialardo, S. Signorelli, L. Gontrani and P. Postorino, *J. Phys. Chem. Solids*, 2015, **84**, 13–16.
- 25 Y. Xu, B. Chen, W. Qian and H. Li, *J. Chem. Thermodyn.*, 2013, **58**, 449–459.
- 26 A. Mariani, O. Russina, R. Caminiti and A. Triolo, *J. Mol. Liq.*, 2015. DOI: 10.1016/j.molliq.2015.10.054
- 27 M. Brehm and B. Kirchner, *J. Chem. Inf. Model.*, 2011, **51**, 2007–2023.
- 28 W. Humphrey, A. Dalke and K. Schulten, *J. Mol. Graph.*, 1996, **14**, 33–38.
- 29 M. Brehm, H. Weber, M. Thomas, O. Hollóczki and B. Kirchner, *ChemPhysChem*, 2015, **16**, 3271–3277.
- 30 D. a Case, T. E. Cheatham, T. Darden, H. Gohlke, R. Luo, K. M. Merz, A. Onufriev, C. Simmerling, B. Wang and R. J. Woods, *J. Comput. Chem.*, 2005, **26**, 1668–88.
- 31 J. Wang, R. M. Wolf, J. W. Caldwell, P. A. Kollman and D. A. Case, *J. Comput. Chem.*, 2004, **25**, 1157–1174.
- 32 J.-P. Ryckaert, G. Ciccotti and H. J. Berendsen, *J. Comput. Phys.*, 1977, **23**, 327–341.
- 33 M. J. Frisch, G. W. Trucks, H. B. Schlegel, G. E. Scuseria, M. A. Robb, J. R. Cheeseman, G. Scalmani, V. Barone, B. Mennucci, G. A. Petersson, H. Nakatsuji, M. Caricato, X. Li, H. P. Hratchian, A. F. Izmaylov, J. Bloino, G. Zheng, J. L. Sonnenberg, M. Hada, M.; Ehara, R. Toyota, K.; Fukuda, J. Hasegawa, M. Ishida, T. Nakajima, Y. Honda, O. Kitao, H. Nakai, T. Vreven, J. Montgomery, J. A., J. E. Peralta, F. Ogliaro, M. Bearpark, J. J. Heyd, E. Brothers, K. N. Kudin, V. N. Staroverov, R. Kobayashi, J. Normand, K. Raghavachari, A. Rendell, J. C. Burant, S. S. Iyengar, J. Tomasi, M. Cossi, N. Rega, M. J. Millam, M. Klene, J. E. Knox, J. B. Cross, V. Bakken, C. Adamo, J. Jaramillo, R. Gomperts, R. E. Stratmann, O. Yazyev, A. J. Austin, R. Cammi, C. Pomelli, J. W. Ochterski, R. L. Martin, K. Morokuma, V. G. Zakrzewski, G. A. Voth, P. Salvador, J. J. Dannenberg, S. Dapprich, A. D. Daniels, Ö. Farkas, J. B. Foresman, J. V. Ortiz, J. Cioslowski, D. J. Fox and I. Gaussian, 2009.
- 34 S. Pronk, S. Páll, R. Schulz, P. Larsson, P. Bjelkmar, R. Apostolov, M. R. Shirts, J. C. Smith, P. M. Kasson, D. Van Der Spoel, B. Hess and E. Lindahl, *Bioinformatics*, 2013, **29**, 845–854.
- 35 L. Gontrani, O. Russina, F. C. Marincola and R. Caminiti, *J. Chem. Phys.*, 2009, **131**, 244503.

Journal Name

COMMUNICATION

- 36 R. Caminiti and V. R. Albertini, *Int. Rev. Phys. Chem.*, 1999, **18**, 263–299.